Solution Properties of Conventional Gum Arabic and a Matured Gum Arabic (*Acacia* (sen) SUPER GUM)

Qi Wang,*,† Walther Burchard,‡ Steve W. Cui,† Xiaoqing Huang,† and Glyn O. Phillips§

Guelph Food Research Center, Agriculture and Agri-Food Canada, Guelph, N1G 5C9, Ontario, Canada, Institut für Makromolekulare Chemie, Albert Ludwigs Universität, 79104 Freiburg i. Br., Germany, Phillips Hydrocolloids Research Centre, The North East Wales Institute, Wrexham LL11 2AW, Wales, United Kingdom, Phillips Hydrocolloids Research Ltd, 45 Old Bond Street, London W1S 4AQ, United Kingdom

Received October 22, 2007; Revised Manuscript Received December 3, 2007

Dilute solution properties of two specially matured gum arabic samples (EM1 and EM2) were compared to the conventional gum (EM0) using static light scattering. The apparent molar mass ($M_{w,app}$) and radius of gyration ($R_{g,app}$) for the three samples showed unusual concentration dependence. These data were satisfactorily interpreted by a simple association model that takes into account the repulsive interaction among clusters, which allowed us to obtain the true molar mass ($M_w(0)$) and radius of gyration ($R_g(0)$). A common power law relation was observed between $M_w(0)$ and $R_g(0)$, giving a somewhat higher exponent than expected for linear and branched polymers in a good solvent. $M_w(0)$ and $R_g(0)$ obtained for the three gums do not differ significantly from each other. However, the data showed clearly a constant increase of the association from EM0 to EM2 with increasing concentration. This is in accordance with the previously observed improved functional properties for the matured products.

Introduction

Acacia gum, which is a food additive approved by the Codex Alimentarius, is defined to be within the *Acacia* subgenus (family Leguminosae). The acacia gum (gum arabic) of commerce (E 414 and INS 414) comes exclusively from the ACACIA Bentham series Gummiferae and series Vulgares. A historic synopsis on the origin and use from ancient times to presence was given by Sanchez et al.[1] Gum arabic is one of the most commonly used hydrocolloids in the food industry due to its excellent emulsifying properties in oil-in-water emulsion type products. *Acacia senegal* (*Acacia senegal* var. senegal) is the best characterized species in the Acacia family and is the subject of this paper. It is a complex polysaccharide containing a small amount of proteinaceous material (~2%).[2] The gum can be fractionated by hydrophobic affinity and size exclusion chromatography into three distinctive components: an arabinogalactan (AG), an arabinogalactan−protein complex (AGP), and a glycoprotein (GP).[3–5] The major component AG represents ~88% of the total gum and contains only less than 1% protein. The AGP component comprises ~10% of the total gum with a larger amount of protein ~12%. AGP is the component that has been believed to be responsible mainly for the emulsifying properties of gum arabic.[6–9] A "wattle blossom-type" structure was proposed[7] where blocks of polysaccharide molecules are linked to a common polypeptide chain.[7–9] The minor component GP represents ~1% of the total gum and contains ~50% protein. The major amino acids are hydroxyproline (27–30.4 mol %[7–9]) and serine (14 −21 mol %[7–9]) in the AGP and AG fractions, whereas aspartic, serine, leucine, and glycine are the main components in the GP fraction.[7] The core polysaccharide structure from all the fractions consists of a β-(1,3)-linked galactose backbone with extensive short chain branching at C6 positions.[2,10] The branches consist of arabinose, galactose, rhamnose, and glucuronic acid. A schematic structure of the polysaccharide component is shown in Figure 1.[11]

Analysis by size exclusion chromatography showed that the molecular weight of the three components differ considerably in an order of $M_{AGP} > M_{AG} > M_{GP}$.[7] It has been recognized that low molecular weight AG and GP components assemble into larger molecular weight AGP during a natural maturation process. Recently, a patented novel process was developed to produce matured gum arabic with greatly improved functionality.[12–15] Studies by NMR analysis gave evidence that the matured gum is chemically identical to the base gum.[16] It was suggested that the improved functionality is a result of redistribution of the three components through a process similar to the natural maturation process which occurs within the tree and which leads to improved emulsifying properties. The process transfers low molecular weight AG and GP components via their protein moieties into the AGP component, which is then in greater amount and of higher molecular weight. The nature of this AGP component is not well understood either in the base gum or in the enhanced gum of higher molecular weight. That is one of the objectives of this paper.

Cowman et al.[17] showed by AFM microscopy that the AG component appeared predominantly as globules on mica or graphite surfaces. However, it is not clear if these globules represented the true structure in the solution because the images could represent the collapsed state from a more extended structure, a result of the drying process. For a better understanding of the structure–function relationships, it is necessary to have knowledge of the solution properties. Our preliminary light scattering measurements revealed that gum arabic exhibited an unusual concentration dependence of molar mass. The observed behavior resembled an associating system with repulsive interactions among the associated clusters. The occurrence of

* Corresponding author. E-mail: wangq@agr.gc.ca. Telephone: +1-519-780-8029.
† Guelph Food Research Center, Agriculture and Agri-Food Canada.
‡ Institut für Makromolekulare Chemie, Albert Ludwigs Universität.
§ Phillips Hydrocolloids Research Centre; Phillips Hydrocolloids Research Ltd.

10.1021/bm7011696 CCC: $40.75
Published on Web 03/07/2008

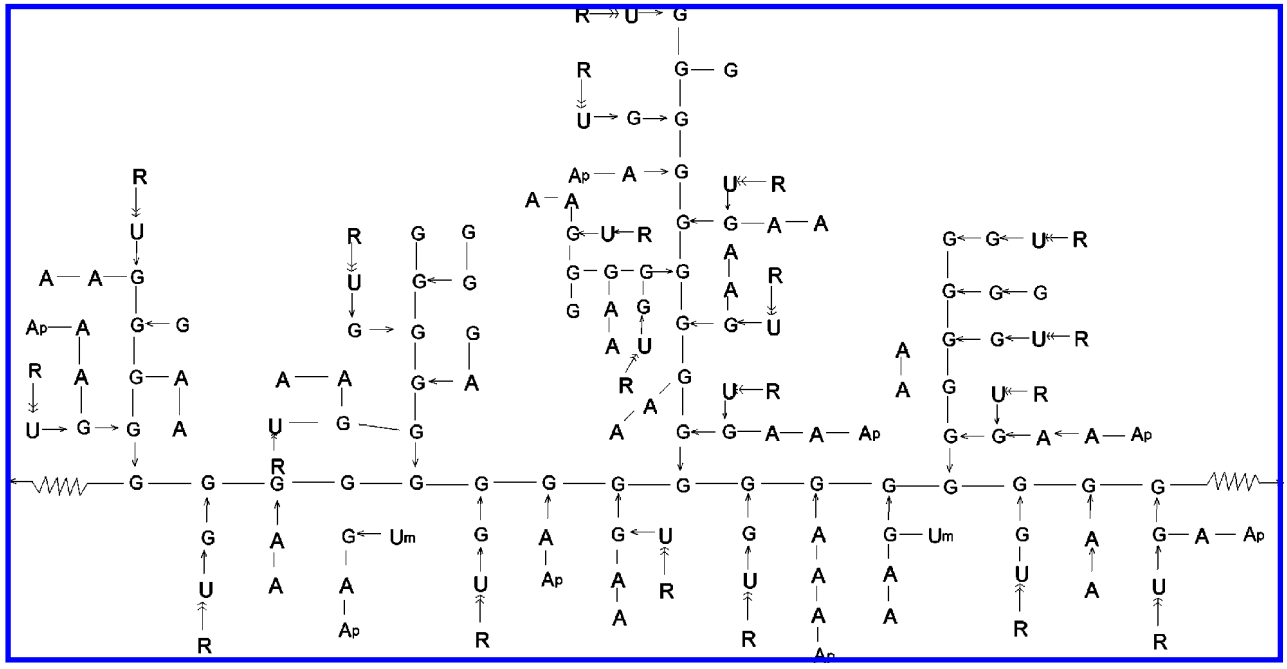

Figure 1. Chemical structure of the polysaccharide components of gum arabic.[11] R, rhamnose; U_m, 4-*O*-methyglucuronic acid; U, glucuronic acid; Ap, arabinopyranose; A, arabinose; and G, galactose.

special, i.e., attracting interactions, which lead to association in combination with nonspecific and repulsive interparticle interactions, requires a description of the presently available theory, which will be outlined in the following section.

Theory. *The Model.* Structure formation through association of colloids was first treated by Smoluchowsky.[18,19] He considered the coagulation process in dilute suspensions as a function of time, being controlled by diffusion of the individual and clustered particles. This kinetic approach could be generalized to equilibrium association and is presently used as a basic tool to describe the growth of filamentous micelles as a function of concentration.[20,21] Early theories neglected the influence of particle–particle interaction and received agreement with experiment only in a fairly restricted low concentration regime.[21–24] Elias[21] introduced the effect of the second virial coefficient and could describe the unusual concentration dependence in the more extended concentration regime. This technique has successfully been applied to several polymer sytems.[25–27]

In our study with modified gum arabic, we observed similar behavior to that predicted by Elias, but in our interpretation we have not confined ourselves to the second virial coefficient but took account of the complete influence of the osmotic modulus $(1/RT)(\partial\pi/\partial c)_{p,T}$. This extension of the theory will allow us to identify a rational interpretation of the scattering data at concentrations up to the overlap concentration. As was pointed out already by Smoluchowsky,[19] the diffusion model, which takes into account association only between two components, can no longer be expected to hold in concentrated solution because the semidilute regime is governed by multibody interactions.

The osmotic modulus is measured by static light scattering (LS) at zero scattering angle (forward scattering)

$$\frac{Kc}{R_{\theta=0}} = \frac{1}{RT}\left(\frac{\partial\pi}{\partial c}\right)_{p,T} \equiv \frac{1}{M_{app}(c)} \qquad (1)$$

and defines the concentration dependence of an apparent molar mass.[28] In this equation, R_θ *is* the Rayleigh ratio of the scattering intensity at scattering angle θ, c the weight concentration, and

Scheme 1. Model of Association

$$M_1 + M_1 \underset{}{\overset{K_1}{\rightleftharpoons}} M_2; \qquad [M_2] = (K[M_1])[M_1]$$

$$M_2 + M_1 \underset{}{\overset{K_2}{\rightleftharpoons}} M_3; \qquad [M_3] = (K[M_1])^2\,[M_1]$$

$$M_{j-1} + M_1 \underset{}{\overset{K_{j-1}}{\rightleftharpoons}} M_j; \qquad [M_j] = (K[M_1])^{j-1}\,[M_1]$$

K is a contrast factor of the scattering power of the dissolved sample over that of the solvent, which is proportional to the square of the refractive index increment dn/dc. The other quantities have the usual meaning. The osmotic pressure can be expanded by a virial series[29]

$$\frac{1}{M_{app}(c)} = \frac{1}{M_w(c)}[1 + 2A_2M_w(c)c + 3A_3M_w(c)c^2 + 4A_4M_w(c)c^3 + \cdots] \qquad (2)$$

which shows the correlation of $M_{app}(c)$ with the weight average of the true molar mass $M_w(c)$ at a finite concentration. The square bracket has to be truncated because, at high concentrations much larger than the overlap concentration, the various coefficients develop alternatingly positive and negative values and eventually diverge. The interaction finally approaches power law behavior.[30] In the following, the value in the square bracket in eq 2 will be abbreviated by $M_w(c)/M_{app}(c)$.

Neglecting initially the interparticle interaction, the association scheme can be expressed by common equilibrium thermodynamics,[20,21] where the symbols in square brackets indicate the number of moles per liter. For the derivation of the right side in Scheme 1, we assumed as first approximation for all processes the same equilibrium constant $K_j = K$.

Concentration Dependence of Molar Mass. The weight concentration is given by the sum over the number of moles per liter $[M_j]$ times the degree of aggregation, j, i.e., $(j[M_j])$, which gives

$$c = M_w(0)[M_1]\sum_{j=1}^{\infty}(K[M_1])^{j-1} = \frac{M_w(0)[M_1]}{(1-K[M_1])^2} \quad (3)$$

and for the weight average molar mass, one has

$$\frac{M_w(c)}{M_w(0)} = \frac{\sum_{j=1}^{\infty} j^2[M_1]}{\sum_{j=1}^{\infty} j[M_1]} = \frac{1+K[M_1]}{1-K[M_1]} \equiv X \quad (4)$$

Eliminating $K[M_1]$ from both equations gives a relationship of the molar mass as a function of the concentration

$$X^2 - 1 = \frac{4K}{M_w(0)}c \quad (5)$$

with X as given by eq 4. Thus the equilibrium constant K is obtained from the slope of $X^2 - 1$ as a function of c. Expressed in terms of the molar mass, one has with eqs 4 and 5

$$M_w(c) = M_w(0)\left(1 + \frac{4K}{M_w(0)}c\right)^{1/2} \quad (6)$$

Evaluation of Interparticle Interaction. Actually, however, the apparent molar mass is measured as a function of concentration. The true molar mass $M_w(c)$ at a given concentration is found by the following procedure. At sufficiently low concentrations, the ratio $M_w(c)/M_{app}(c)$ becomes 1, or in other words, when the distance to neighbored particles becomes much larger than the particle diameter, the interactions are no longer significant. Therefore, from the initial points of measurements and the molar mass at $c = 0$, the aggregation number X (or true molar mass) in this region can be obtained. With these first data, the equilibrium constant is found from the initial slope of the plot of $X^2 - 1$ as a function of c. Knowing the equilibrium constant and the molar mass $M_w(0)$ at infinite dilution, $M_w(c)$ can be calculated from eq 6. Furthermore, the ratio $M_w(c)/M_{app}(c) = [M_w(c)/RT][\partial\pi/\partial c)]_{p,T}$ can be evaluated as a function of c.

Apparent and True Radius of Gyration. If only the initial part of the angular dependent scattering intensity is considered, the scattering behavior is given according to the Debye relationship

$$\frac{Kc}{R_\theta(c)} = \frac{1}{M_w(c)} + \frac{1}{3}\frac{R_g^2(c)}{M_w(c)}q^2 + 2A_2c + 3A_3c^2 + 4A_4c^3 \quad (7)$$

with

$$q = \frac{(4\pi n)}{\lambda_0}\sin(\theta/2) \quad (7a)$$

where n is the refractive index of the solvent, λ_0 the wavelength of the used light in vacuum, and θ the scattering angle. The mean square radius of gyration of the nonassociated particle is determined by the slope of the q^2 dependent scattering curve times $3M_w(c = 0)$. The product $R_g q$ is a dimensionless parameter and has universal character, i.e., experimental data from small-angle X-ray (SAXS) or small-angle neutron scattering (SANS) can be used together with those from light scattering. The constant K in eq 7 is an optical contrast factor that depends on the refractive index increment.

At $q^2 = 0$ the expression is $1/M_{app}(c)$, and with this eq 7 can be rearranged, giving

$$\frac{Kc}{R_\theta(c)} = \frac{1}{M_{app}(c)} + \frac{1}{3}\frac{R_g^2(c)}{M_w(c)}q^2 \quad (8)$$

The apparent mean square radius of gyration is now defined by the slope times $3M_{app}(c)$, which leads to

$$R_g^2(c) = R_{g,app}^2(c)\frac{M_w(c)}{M_{app}(c)} \quad (9a)$$

or

$$R_g(c) = R_{g,app}(c)\left(\frac{M_w(c)}{M_{app}(c)}\right)^{1/2} \quad (9b)$$

For nonassociating polymers in a good solvent, there is no change in $R_g(c)$ with the concentration, and this indeed was observed for up to three times the overlap concentration.[29]

Experimental Section

Materials. A commercial gum arabic (*Acacia senegal*) (EM0) and two matured gums (*Acacia* (sen) SUPER GUM, EM1 and EM2, were kindly provided by San-Ei Gen FFI, Inc., Japan. The modification process was described in detail previously.[12,14] Essentially, the gums in the dry state are subjected to a heating process under specially controlled conditions. Some of the physical properties of the samples used are listed in Table 1.

Sample Characterization. *Refractive Index Increment dn/dc.* The dn/dc of gum was measured using a differential refractometer (Brookhaven Instruments Corporation, Holtsville, NY) at a wavelength of 532 nm and 25 °C. The calibration of the refractometer was conducted by running KCl aqueous solutions with concentrations ranging from 1 to 5 mg/mL. Stock polysaccharide solutions at a concentration of 5 mg/mL were made in 0.2 M NaCl aqueous solutions. Six dilutions ranging from 0.1 to 5 mg/mL were prepared for each sample. All the prepared solutions were filtered through a 0.45 μm filter before each measurement was carried out. A static mode of Differential Refractometer Software (Brookhaven Instruments) was used for data acquisition and calculation.

Protein Content. This was determined using a nitrogen analyzer (FP 2000 Leco Instrument UK Ltd., Stockport, Cheshire, UK). The sample (20–30 mg) was combusted in a sealed furnace, and the N content was determined. Measurements were validated by analyzing four standard compounds, atropine (4.84% N), DL-methionine (9.39% N), acetanilide (10.36% N), and nicotinamide (22.94% N) and by running blank and standard samples prior to the actual sample analysis. A factor of 6.25 was used to calculate the protein content.

Light Scattering Measurement. Stock gum solutions (~5 mg/mL) were made by dispersing the samples in 0.2 M sodium chloride water solution at room temperature for about 12 h under constant gentle stirring. The stock solution was filtered five times using a 0.45 μm pore size syringe filter. A series of four lower concentration solutions were made using the same solvent that had been optically clarified by passing through a 0.1 μm filter for five times. Finally, each solution was then filtered directly into a light scattering cell through a 0.45 μm

Table 1. Some Physical Chemical Properties of Gum Arabic (EM0) and *Acacia* (sen) SUPER GUMs (EM1 and EM2)

samples	EM0	EM1	EM2
average M_w[a]	6.22×10^5	1.66×10^6	2.54×10^6
M_w of AGP[a]	2.54×10^6	8.56×10^6	1.16×10^7
M_w of AG[a]	3.96×10^5	4.16×10^5	4.50×10^5
$[\eta]$ dL/g[b]	0.182	0.194	0.216
dn/dc mL/g	0.139	0.142	0.141
protein (dry matter %)	2.42	2.63	2.54

[a] The molecular weight M_w was determined by SEC-MALLS detection.[12] [b] Intrinsic viscosity $[\eta]$ was measured by GPC with a Viscotek triple detector as described previously.[31]

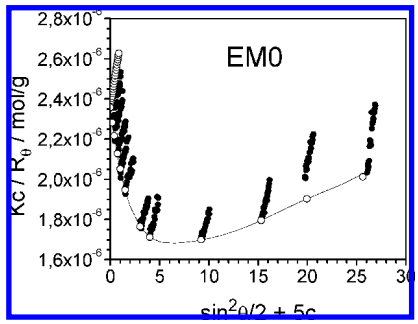

Figure 2. Zimm plot of sample EM0 in 0.2 M NaCl water solution.

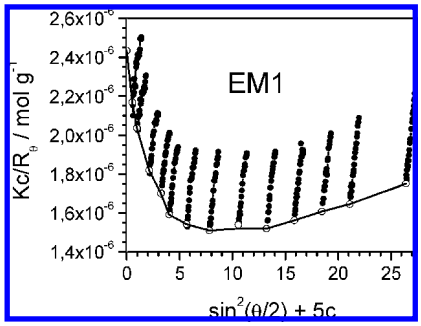

Figure 3. Zimm plot of sample EM1 in 0.2 M NaCl water solution.

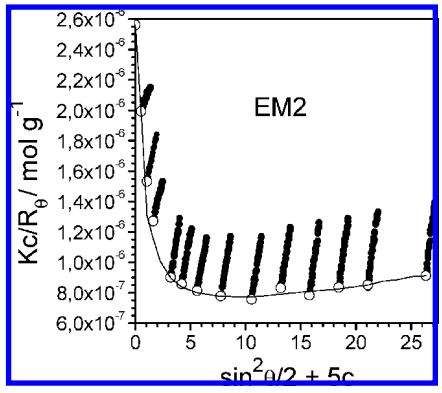

Figure 4. Zimm plot of sample EM2 in 0.2 M NaCl water solution.

filter. All sample preparations were carried out in a hood with vertical laminar flow of filtered air.

Static light scattering measurements were performed at 21 °C using a Brookhaven system including a BI-200SM multiangle motorized goniometer, a BI-APD detector, and a BI-9000AT digital correlator (Brookhaven Instruments). The light source was a 35 mW vertical polarized He-Ne laser of wavelength 633 nm (Melles Criot Laser Group, Carlsbad, CA). The instrument was calibrated using well filtered toluene with a known Rayleigh ratio of 1.398×10^{-5} cm^{-1}. The scattering angles detected ranged from 30 to 150° in steps of 10°.

Results

Protein analysis showed that the two matured gums EM1 and EM2 contained the same level of protein as the original gum arabic EM0 (Table 1). The measured refractive index increments for the three gum samples were also closely similar, $dn/dc = 0.141 \pm 0.002$ mL/g (Table 1), which is in good agreement with literature values obtained for gum arabic.[32,33]

Static light scattering was carried out for the three gum samples (EM0, EM1, and EM2) in the concentration regime from 0 to 5.25 g/L. The corresponding Zimm plots are shown in Figures 2−4. The data at $q = 0$ (forward scattering) represent the reciprocal apparent molar mass ($1/M_{app}$) as a function of concentration. M_{app} showed a complex concentration dependence, and the corresponding values are given in Tables 2−4. The apparent radii of gyration, which were found from the slopes of the q^2 dependent scattering curves timed by $3M_{app}(c)$, i.e., $R_{g,app}(c) = [3M_{app}(c) \times \text{slope}]^{1/2}$, also showed a concentration dependence. The tables also contain the true molar mass $M_w(c)$ and the true radius of gyration $R_g(c)$, which were calculated using the model as described in the Theory Section. The procedure for obtaining these true molecular parameters is outlined as follows.

Table 2. Experimental Data from Gum Arabic EM0 of Apparent Molar Mass and Apparent Radius of Gyration and the Corresponding Results after Correction for the Interparticle Interaction

c (g L^{-1})	$M_{app}(c)/10^6$ (g mol^{-1})	$R_{g,app}(c)$ (nm)	$M_w(c)/10^6$ (g mol^{-1})	$R_g(c)$ (nm)
0	0.4245	24.2	0.4245	24.2
0.0413	0.4386	22.4	0.4394	22.4
0.0801	0.452	21	0.4524	21
0.14	0.469	18.9	0.477	19
0.2	0.4905	20.8	0.4928	20.8
0.301	0.5118	18.9	0.5252	19.1
0.601	0.50.53	20.4	0.6001	21
0.801	0.5659	22.3	0.6531	23.7
1.84	0.579	19.7	0.8625	23.9
3.001	0.5976	23.6	1.1073	32.7
3.95	0.4968	23.1	1.1269	34.8
5.21	0.4921	29.9	1.3491	49.5

Table 3. Experimental Data from Gum Arabic EM1, Apparent Molar Mass, and Apparent Radius of Gyration and the Corresponding Data after Correction for the Interparticle Interaction

c (g L^{-1})	$M_{app}(c)/10^6$ (g mol^{-1})	$R_{g,app}(c)$ (nm)	$M_w(c)/10^6$ (g mol^{-1})	$R_g(c)$ (nm)
0	0.4108	24.6	0.4108	24.6
0.16	0.4609	28.7	0.4715	29
0.191	0.4012	25.9	0.4824	25.7
0.422	0.5496	30.2	0.5567	30.4
9.643	0.5882	32.1	0.6196	31.9
0.8	0.6285	34.6	0.6606	35.7
1.13	0.6485	35.8	0.7394	38.2
1.56	0.6631	37.1	0.831	41.5
2.11	0.5498	36.8	0.9352	43.9
2.64	0.6585	37.4	1.0256	46.7
3.17	0.6201	35.7	1.1087	46.8
3.69	0.6223	35.8	1.1845	49.4
4.22	0.6081	36.8	12.571	52.9
5.28	0.5715	36.4	1.391	56.8

Table 4. Experimental Data from Gum Arabic EM2, Apparent Molar Mass, and Apparent Radius of Gyration and the Corresponding Results after Correction for the Interparticle Interaction

c (g L^{-1})	$M_{app}(c)/10^6$ (g mol^{-1})	$R_{g,app}(c)$ (nm)	$M_w(c)/10^6$ (g mol^{-1})	$R_g(c)$ (nm)
0	0.3905	22.2	0.3905	22.2
0.105	0.5019	20.5	0.5545	21.5
0.211	0.6529	31.2	0.6812	31.9
0.322	0.7869	33.1	0.7925	32.1
0.642	1.1114	46.8	1.049	45.5
0.843	1.1664	45.6	1.189	45.9
1.12	1.2294	45.2	1.3439	47.3
1.55	1.2867	49.9	1.5637	54.9
2.11	1.3239	51.6	1.8076	60.3
2.64	1.2051	48.8	1.8209	69
3.16	1.2794	53.9	2.1388	69.8
3.69	1.1985	51.9	2.2419	71
4.22	1.1753	52.5	2.5413	77.2
5.27	0.8277	45.7	2.6828	82.3

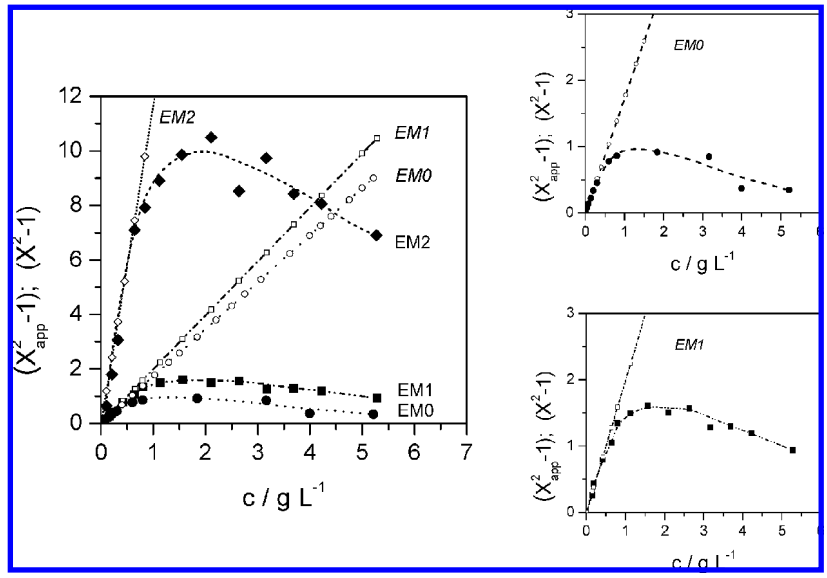

Figure 5. Concentration dependence of degree of association (X) for samples EM0, EM1, and EM2. Solid symbols are calculated from static light scattering experiment data via eq 4 ($X^2_{app} - 1$). Open symbols are the linear fit of the initial data points ($X^2 - 1$). The slope of the curves gives the equilibrium constants for the three samples.

Molar Mass $M_w(c)$. To a reasonable approximation, we can assume negligible influence of the interparticle interaction on the measured reciprocal molar mass when the concentration $c = 0$ is approached. Therefore, in the very dilute regime, the measured data of $1/M_{app}(c)$ should approach the true reciprocal molar mass, $1/M_w(c)$. In this regime, the degree of association $X = M_w(c)/M_w(0)$ is related to the concentration by eq 5. Figure 5 shows a plot of $(X^2_{app} - 1)$ as a function of c. The initial part can be well approximated by a straight line whose slope is $4K/M_w(0)$, where $M_w(0) = M_{app}(c = 0)$. With this initial slope in Figure 5 and the molar mass of the nonassociated unimer, $M_w(0)$, the true molar mass at each concentration $M_w(c)$ can be calculated applying eq 6 (Tables 2−4). The association constants were found to be $K_{EM0} = 8.3 \times 10^5$, $K_{EM1} = 20.4 \times 10^5$, and $K_{EM2} = 97.8 \times 10^5$ mol^{-1}, which are in the order $K_{EM2} > K_{EM1} > K_{EM0}$. These values are consistent with the aggregation mechanism, which was proposed for the formation of the SUPER GUM series of products and indicate that even in its natural state there is association occurring in gum arabic.

Interparticle Interaction or Osmotic Modulus. According to eqs 1 and 2, the interparticle interaction is defined by the ratio

$$\frac{M_w(c)}{M_{app}(c)} = \frac{M_w(c)}{RT}\left(\frac{\partial \pi}{\partial c}\right)_{p,T} \qquad (10)$$

Figure 6 shows the concentration dependence of $1/M_{app}(c)$ and of $1/M_w(c)$ as a function of c. From the ratio of these two quantities, the reduced osmotic modulus is derived. The concentration dependence of osmotic modulus is shown in Figure 7.

Radius of Gyration $R_g(c)$. Having determined the interparticle interaction function, the true radius of gyration $R_g(c)$ can be calculated with eq 9b from the measured apparent radius of gyration $R_{g,app}(c)$. The result is shown in Figure 8.

Association Phenomena. The increasing association tendency from EM0 to EM2 is clearly seen from Figures 5 and 6 as well as from the association constant K. All three samples show approximately the same molar mass $M_w = 404000 \pm 3000$ g/mol at zero concentration. Despite the large difference in the magnitude of the association constants, the interparticle interaction exhibits similar concentration dependence (see Figure 7).

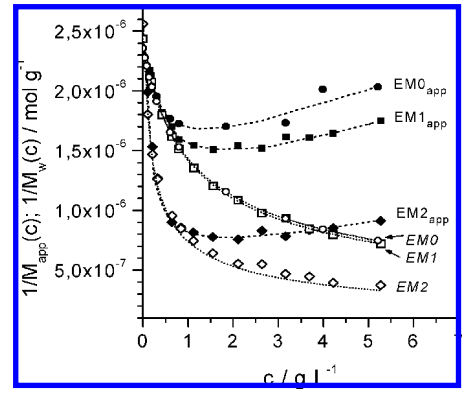

Figure 6. Concentration dependence of apparent reciprocal molar mass $1/M_{app}(c)$ (solid symbols) and true reciprocal weight average molar mass $1/M_w(c)$ (open symbols) for the three samples EM0 (circle), EM1 (square), and EM2 (diamond).

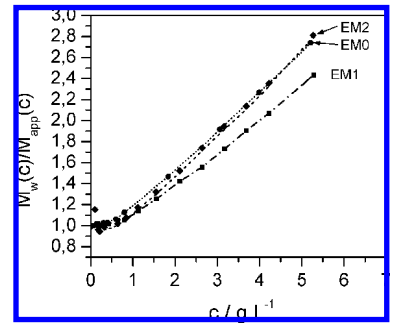

Figure 7. Reduced osmotic modulii as functions of concentration for the three gum arabic samples EM0 (circle), EM1 (square), and EM2 (diamond).

As expected, the concentration dependence of the radii of gyration (Figure 8) also indicates growth of the particle dimensions with the concentration, i.e., with the degree of aggregation. Surprisingly, the conventional gum arabic EM0 exhibited at first a shrinking of dimensions, and only at higher concentrations a similar increase in size became evident.

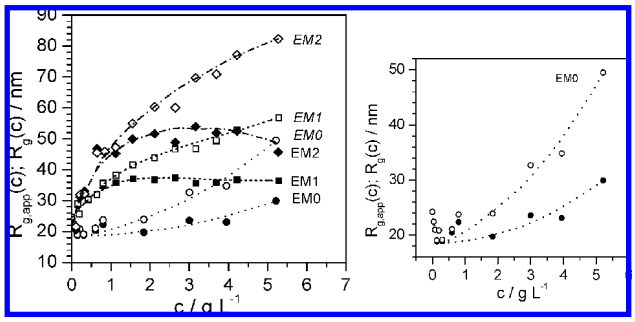

Figure 8. Concentration dependence of apparent radii of gyration $R_{g,app}(c)$ (solid symbol) and true radii of gyration $R_g(c)$ (open symbol) for samples EM0 (circle), EM1 (square), and EM2 (diamond).

Finally, the molar mass dependencies of the apparent radius of gyration and true radius of gyration are shown in parts a and b of Figure 9, respectively. Again, the difference between the modified and original arabic gums is apparent. The unexpected correlation between the apparent molar mass and radius of gyration (Figure 9a) is converted to a more common power law behavior for the true parameters, $R_g(c)$ and $M_w(c)$ (Figure 9b), that is, when the influence of the particle–particle interactions has been eliminated. In all three cases, the power law behavior is observed, and only for EM0 is the power law preceded by an initial decrease in dimension although the molecular weight is slightly increased.

Discussion

Our study of the gum arabic solution properties reveals for all three gums evidence of association in aqueous solutions. Using the theory for the simple model of open association, it was possible to derive the true molar molecular parameters from the measured apparent values. The concentration dependencies of the apparent and true molecular parameters were found to be significantly different. For the two modified gums, the apparent radius of gyration at first increased with the concentration, passed through a maximum, and then decreased again (Figure 8). Similar behavior was observed for the apparent molar mass. This unusual behavior disappeared when the interparticle interaction was taken account in application of the association model. The obtained power law dependence between the calculated true molar mass and true radius of gyration is in agreement with most common polymers. This result would seem to justify our approximation in the application of the simplified model. The exponents obtained for the three gums were somewhat higher than those for linear and branched chains in a good solvent, which should be less than 0.58 and also slightly increased with maturation. These high exponents would signify stiffness of the molecules. Support for rodlike behavior of a component of these samples came also from recent small-angle X-ray scattering measurements by Cohen et al.,[34] who in the dilute regime found a mass fractal dimension of close to 1 and a 4 nm cross-sectional diameter for the rodlike particles. However, the high exponents could also result from an increasing polydispersity in the course of association. The mean square radius of gyration is a z-average ($\langle R_g^2 \rangle_z$), whereas the molar mass is a weight average; the former increases more strongly with the polydispersity than the weight average $M_w(c)$. At the present stage, we cannot make a clear statement of which interpretation is the most appropriate. We repeat a comment that the simple model can only hold for dilute solutions. Smoluchowsky's derivation is based on mutual diffusion and includes the assumption that the coagulation occurs one by one at each step between two particles, which essentially will produce a linear assembly. In the range of the overlap concentration, this assumption no longer remains valid. This comment by Smoluchowsky[20] stimulated us to extend our measurements to much higher concentrations. The work is still ongoing, and results will be reported later. We expect to receive valuable information from these additional measurements, which will allow us to set up a more detailed mechanism for the association.

The behavior of unmodified gum requires special consideration. Unlike the modified gums, the radius of gyration decreased initially with concentration while the molar mass slightly increased with the concentration (Figures 8 and 9). This unexpected behavior has also been observed with a few other polymers and has been attributed to intraparticle interactions.[25,26] This intraparticle interaction was dominant at low concentration regime and changed to common association at higher concentrations. In the currently applied model, we only took into account the *inter*particle interactions, i.e., the specific-attractive and nonspecific-repulsive ones. It was the specific *intra*particle interactions which caused such more complex behavior.

At this stage, we are not able to make a definite suggestion of which structure elements may cause the interparticle interaction; nonetheless, we were able to separate the effect of nonspecific repulsive interaction from the actual structure properties and obtained a reasonable result. From the current study, it is obvious that the two modified gums have greater potential for association than the unmodified gum, which

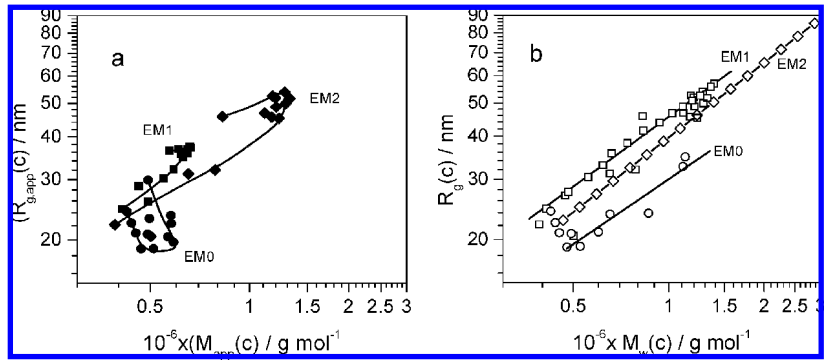

Figure 9. Molar mass dependence of the radii of gyration for samples EM0 (circle), EM1 (square), and EM2 (diamond) (a) for the apparent, experimentally measured data, (b) for the derived true radii of gyration $R_g(c)$ and molar mass $M_w(c)$. The curves follow the power law behavior: $R_g(c) = 1.48 \times 10^{-5}\ M_w(c)^{0.63}$ (EM0), $R_g(c) = 4.56 \times 10^{-5}\ M_w(c)^{0.68}$ (EM1), and $R_g(c) = 3.97 \times 10^{-5}\ M_w(c)^{0.72}$ (EM2).

nevertheless shows the same tendency. It is reasonable that it is the longer proteinaceous component that plays an important role in the association of gum arabic molecules. In the AGP component, the polysaccharide moiety is attached to the polypeptide chain through hydroxyproline,[7–9] which is abundant in natural polypeptide chains. Probably, the balance of hydrophobicity and hydrophilicity controls the association phenomena that we observe. The aggregation which follows the heat treatment changes the overall shape, possibly due to conformational changes of the polypeptide chains which make the reactive regions more available for association. Size exclusion chromatography has shown that the AGP fraction increased from 10% in the control gum to 18% in EM2.[13] Our results are consistent with an increased aggregation tendency most likely to be associated with the greater proportion of the AGP fraction. Because the predominant amino acids in the AGP are hydroxyproline and serine, hydrogen bonding may also contribute to the intermolecular association in addition to hydrophobic forces.

Conclusion

Static light scattering data from an unmodified (EM0) and two matured gum arabic (EM1, EM2) samples can be interpreted by a simple association model that takes into account the repulsive interaction among clusters. The model allowed us to obtain the true molar mass and radius of gyration of the samples studied after correction for the repulsive interaction among the particles. At zero concentration, the true molar mass of the gums do not differ significantly from each other. However, the data showed clearly a continuous increase of the association from EM0 to EM2, which may account for the improved functional properties and is consistent with the previously proposed aggregation mechanism for the formation of the SUPER GUM products by the heating process.

References and Notes

(1) Sanchez, C.; Renard, D.; Robert, P.; Schmitt, C.; Lefevre, J. *Food Hydrocolloids* **2002**, *16*, 257–267.
(2) Clarke, A. E.; Anderson, R. L.; Stone, B. A. *Phytochemistry* **1978**, *18*, 521–540.
(3) Randall, R. C.; Phillips, G. O.; Williams, P. A. *Food Hydrocolloids* **1989**, *3*, 65–75.
(4) Vandevelde, M.-C.; Fenyo, J. C. *Carbohydr. Polym.* **1985**, *5*, 251–273.
(5) Connolly, S.; Fenyo, J. C.; Vandevelde, M.-C. *Carbohydr. Polym.* **1988**, *8*, 23–32.
(6) Randall, R. C.; Phillips, G. O.; Williams, P. A. *Food Hydrocolloids.* **1988**, *2*, 131–140.
(7) Williams, P. A.; Phillips, G. O. In *Handbook of Hydrocolloids*; Phillips, G. O. Williams, P. A., Eds.; CRC Press: New York, 2000, pp 155–168..
(8) Akiyama, Y.; Eda, S.; Kato, K *Agric. Biol. Chem* **1984**, *48*, 235–237.
(9) Wu, Q.; Fong, C.; Lampert, D. T. A. *Plant Physiol.* **1991**, *96*, 848–855.
(10) Anderson, D. M. W.; Hirst, E. V.; Stoddart, J. F. *J. Chem. Soc.* **1967**, 1476–1486.
(11) Street, C. A.; Anderson, D. M. W. *Talanta* **1983**, *30*, 887–893.
(12) Al-Assaf, S.; Phillips, G. O.; Aoki, H.; Sasaki, Y. *Food Hydrocolloids* **2007**, *21*, 319–328.
(13) Aoki, H.; Katayama, T.; Ogasawara, T.; Sasaki, Y.; Al-Assaf, S.; Phillips, G. O. *Food Hydrocolloids* **2007**, *21*, 353–358.
(14) Aoki, H.; Katayama, T.; Al-Assaf, S.; Phillips, G. O. *Food Hydrocolloids* **2007**, *21*, 329–337.
(15) Pickles, N. A.; Aoki, H.; Al-Assaf, S.; Sakata, M.; Ogasawara, T.; Ireland, H. E.; Coleman, R. C.; Phillips, G. O.; Williams, J. H. H. *Food Hydrocolloids* **2007**, *21*, 338–346.
(16) Cui, S. W.; Phillips, G. O.; Blackwell, B.; Nikiforuk, J. *Food Hydrocolloids* **2007**, *21*, 347–352.
(17) Cowman, M. K.; Funami, T.; Al-Assaf, S.; Kudasheva, D. S.; Mohan, D.; Phillips, G. O. *Foods Food Ingredients J. Jpn.* **2006**, *211*, 207–212.
(18) Smoluchowsky, v.M. *Phys. Z.* **1916**, *17*, 585–599, 557–571.
(19) See also (a) Chandrasekhar, S. *Rev. Mod. Phys.* **1943**, *15* (III.6), 59–63. (b) Wax, E., Ed. *Selected Papers on Noise and Stochastic Processes*; Dover Publications: New York. 1954; pp 1–89.
(20) Hunter, R. J. *Foundations of Colloidal Science*; Oxford University Press: Oxford, 1989; Vol. 1, Chapter 10.3, pp 577–583..
(21) (a) Elias, H.-G.; Solc., K. *Makromol. Chem.* **1975**, *176*, 365–372. (b) Huglin M. In *Light Scattering from Polymer Solutions*; Academic Press: London 1972; Chapter 9, pp. 397–457.
(22) Hoffmann, H.; Löbl, M.; Rehage, H. In Degiorio, V., Corti, M., Eds. *Physics of Amphiphiles, Micelles, Vesicles and Microemulsions*; North Holland: Amsterdam, 1985; pp 237–259..
(23) Corti, M. In Degiorio, V., Corti, M., Eds. *Physics of Amphiphiles, Micelles, Vesicles and Microemulsions*, North Holland, Amsterdam 1985, p. 122–157..
(24) (a) Sund, H.; Markau, K *Int. J. Polym. Matter* **1976**, *4*, 250. (b) Burchard, W. *Trends Polym. Sci.* **1993**, *1*, 192–198.
(25) Pedley, A. M.; Higgins, J. S.; Peiffer, D. G.; Burchard, W. *Macromolecules* **1990**, *23*, 1434–1437.
(26) Phoon, C. L.; Higgins, J. S.; Burchard, W.; Peiffer, D. G. *Macromol. Rep.* **1992**, *A29* (Suppl. 2), 179–188.
(27) Bongaerts, K.; Paoletti, S.; Denef, B.; Varneste, K.; Cuppo, F.; Reynaers, H. *Macromolecules* **2000**, *33*, 8709–8719.
(28) Burchard, W. In Roovers, J., Ed. *Branched Polymers II*; Advances in Polymer Science; Springer-Verlag:New York, 1999; Vol. 143, Section 8.3, pp 113–194.
(29) Burchard, W. *Biomacromolecules* **2001**, *2*, 342–353.
(30) De Gennes, P.-G. *Scaling Concepts in Polymer Physics*; Cornell University Press: Ithaca, NY, 1979.
(31) Wang, Q.; Huang, X.; Nakamura, A.; Burchard, W.; Hallett, F. R. *Carbohydr. Res.* **2005**, *340*, 2637–2644.
(32) Randall, R. C.; Phillips, G. O.; Williams, P. A. *Food Hydrocolloids* **1989**, *3*, 65–75.
(33) Lewis, B. A.; Smith, F. *J. Am. Chem. Soc.* **1957**, *79*, 3929–3931.
(34) Cohen, Y.; Rafail, L.; Dror, Y.; Schmitt, J.; Talmon, Y. Presented at *2nd International Hydrocolloids Forum: Natural Hydrocolloid Emulsifier*, Wrexham, UK, 2007. We wish to express our thanks to the authors for referring to these data prior to publication.

BM7011696